GPS Solut (2009) 13:23–34
DOI 10.1007/s10291-008-0094-z

ORIGINAL ARTICLE

Antenna phase center calibration for precise positioning of LEO satellites

Oliver Montenbruck · Miquel Garcia-Fernandez · Yoke Yoon · Steffen Schön · Adrian Jäggi

Received: 10 January 2008 / Accepted: 19 May 2008 / Published online: 7 June 2008

Abstract Phase center variations of the receiver and transmitter antenna constitute a remaining uncertainty in the high precision orbit determination (POD) of low Earth orbit (LEO) satellites using GPS measurements. Triggered by the adoption of absolute phase patterns in the IGS processing standards, a calibration of the Sensor Systems S67-1575-14 antenna with GFZ choke ring has been conducted that serves as POD antenna on various geodetic satellites such as CHAMP, GRACE and TerraSAR-X. Nominal phase patterns have been obtained with a robotic measurement system in a field campaign and the results were used to assess the impact of receiver antenna phase patterns on the achievable positioning accuracy. Along with this, phase center distortions in the actual spacecraft environment were characterized based on POD carrier phase residuals for the GRACE and TerraSAR-X missions. It is shown that the combined ground and in-flight calibration can improve the carrier phase modeling accuracy to a level of 4 mm which is close to the pure receiver noise. A 3.5 cm (3D rms) consistency of kinematic and reduced dynamic orbit determination solutions is achieved for TerraSAR-X, which presumably reflects the limitations of presently available GPS ephemeris products. The reduced dynamic solutions themselves match the observations of high grade satellite laser ranging stations to 1.5 cm but are potentially affected by cross-track biases at the cm-level. With respect to the GPS based relative navigation of TerraSAR-X/TanDEM-X formation, the in-flight calibration of the antenna phase patterns is considered essential for an accurate modeling of differential carrier phase measurements and a mm level baseline reconstruction.

Keywords Antennas · Phase center variation · Orbit determination · LEO satellites · TerraSAR-X · CHAMP · GRACE

O. Montenbruck (✉) · M. Garcia-Fernandez · Y. Yoon
German Space Operations Center, Deutsches Zentrum für Luft- und Raumfahrt, 82230 Weßling, Germany
e-mail: oliver.montenbruck@dlr.de

S. Schön
Institut für Erdmessung, Leibniz Universität Hannover, 30167 Hannover, Germany

A. Jäggi
Astronomisches Institut der Universität Bern, Sidlerstrasse 5, 3012 Bern, Switzerland

Introduction

Global positioning system (GPS) sensors are well recognized today as a key tracking system for precise orbit determination (POD) of satellites in low Earth orbit (LEO). Sub-decimeter position accuracies have first been demonstrated in the TOPEX/Poseidon and CHAMP missions. More recently, radial accuracies of about 1 cm have been achieved for Jason-1 (Haines et al. 2004) and GRACE (Kang et al. 2006, Jäggi et al. 2007) in GPS-only reduced dynamic orbit determinations.

The BlackJack receiver and its commercial IGOR (integrated GPS and occultation receiver) version that are most widely used for geodetic grade space missions exhibit a representative noise level of 1 mm for L1 and L2 carrier phase measurements, or, equivalently, 2–3 mm for the ionosphere-free L1/L2 combination (Montenbruck et al. 2006). In order to fully exploit this accuracy level, a careful modeling of antenna phase center offsets and variations is required. This is particularly true for precise point

positioning (PPP) solutions, which do not benefit from the dynamical constraints imposed by a physical trajectory model. Besides a larger overall scatter, these purely kinematic orbit determination solutions are likely to be affected by biases as a result of small systematic measurement modeling uncertainties.

With the introduction of absolute phase patterns in the processing standards of the international GNSS service (IGS) and the availability of calibrated receiver and transmitter antenna patterns (Schmid et al. 2005, 2007) terrestrial PPP users can now benefit from improved GPS orbit and clock products and a refined carrier phase modeling. On the other hand, concise receiver antenna phase patterns are unavailable for many space missions or have commonly been neglected in the routine processing.

The present study therefore addresses the impact of receiver phase center offsets and variations on the orbit determination of low Earth satellites. It focuses on the TerraSAR-X mission which carries an IGOR GPS receiver and employs a Sensor Systems S67-1575-14 patch antenna along with a choke ring manufactured by the GeoForschungsZentrum (GFZ) Potsdam. The same antenna system and nearly identical receivers are used onboard the CHAMP satellite, the GRACE twins and the TanDEM-X satellite that will establish a close formation with TerraSAR-X from 2009 onwards.

Key contributions of this study comprise the field and in-flight calibration of the aforementioned antenna and choke ring combination and a critical assessment of benefits and limitations of both techniques. It is demonstrated that notable distortions of the phase pattern may exist even in a presumably benign spacecraft environment. Application of both ground and in-flight calibrated phase patterns within the precise orbit determination is shown to clearly reduce the difference between kinematic and reduced dynamic solutions as well as the goodness-of-fit of the carrier phase measurements.

The paper starts with a description of the antenna system and the automated field calibration using a robotic measurement system. The average phase pattern and the variation among different antenna samples are discussed. In a second step, the estimated phase center offsets and pattern are applied in the orbit determination process and the results are compared against solutions considering only the antenna reference point (ARP) or the mean phase centers for each frequency. Based on the observed carrier phase residuals an empirical phase center correction map is constructed and introduced into the orbit determination. Independent results are obtained for the two POD antennas and compared along with an assessment of the achieved orbit determination accuracy.

Field calibration

Antenna system description

The Sensor Systems S67-1575-14 GPS antenna is a passive dual-frequency patch antenna that was originally designed and qualified for aeronautical applications. As part of the CHAMP and GRACE project, thermal-vacuum tests and outgassing tests have been conducted by JPL (C. Dunn, priv. comm.) to qualify the antenna for use in a space environment. The antenna has, furthermore, undergone vibration testing after spacecraft integration to ensure its proper operation after launch. A dedicated lightweight choke ring for use in satellite missions has been manufactured by GFZ. The resulting antenna/choke ring combination (which will henceforth be designated as S67-1575-14+CRG, with CRG indicating the GFZ choke ring) is employed both on CHAMP and GRACE, as well as the TerraSAR-X and TanDEM-X satellites.

As a non-geodetic antenna, the S67-1575-14 design imposes no dedicated specifications for phase center location and stability. Phase pattern information is presently unavailable in the IGS antenna database (ftp://igscb.jpl.nasa.gov/pub/station/general/igs05_1473.atx) due to its non-use in the global ground network. Calibrations performed in 1997 by the National Geodetic Survey (NGS, see http://www.ngs.noaa.gov/cgi-bin/query_cal_antennas.prl?Model=SEN&Antenna=SEN67157514,CR) are based on a notably different choke ring, limited to elevation angles above 10° and ignore a possible azimuth variation. An independent calibration was therefore deemed necessary. In fact, the results described later exhibit significant differences in the ARP location (21 mm in L1, 4 mm in L2 for the up-component) and PCV (up to 2 mm), which renders the NGS values useless for our purposes.

In preparation for a field calibration an ARP and coordinate system has been assigned to the antenna, which is illustrated in Fig. 1. The positive z axis ("Up") coincides with the mechanical symmetry axis and points along the boresight direction. Its intersection with the bottom side of the patch antenna defines the origin of the coordinate system and serves as ARP. The y axis ("North") points from the origin to the center of the mounting hole next to the name plate (serial number label) and the x axis ("East") completes a right-handed coordinate system. For consistency with adopted standards for terrestrial antennas and phase pattern descriptions in a North–East-Up reference system (cf. Rothacher and Schmid 2006), the azimuth angle is counted in a clock-wise (left-handed) sense from the y axis to the x axis. Other than for terrestrial antennas, however, the adopted ARP does not coincide with the bottom of the antenna assembly but is located at the top surface of the choke ring. This is consistent with the

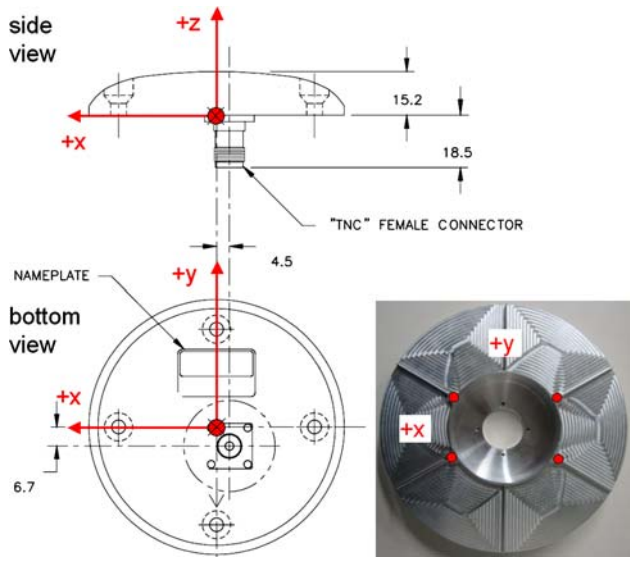

Fig. 1 Definition of the antenna reference point and axes for the S67-1575-14+CRG phase center calibration (outline drawing from Sensor Systems, 2003). In the *lower right corner* the *bottom side* of the choke ring is shown with the associated axes orientation

Fig. 2 The IfE robotic measurement system for the automated absolute field calibration with the CHAMP/GRACE/TerraSar-X GPS antenna

definition of the mechanical reference point for the antenna established by the spacecraft manufacturer.

Calibration campaign

The S67-1575-14+CRG phase center offset and variation were determined using the Automated Absolute Field Calibration Technique that has jointly been developed by the Institut für Erdmessung (IfE) and Geo++ (Wübbena et al. 2000). The device under test is mounted on a well calibrated robot that performs rapid tilts and rotations of the antenna. While individual measurements are strongly affected by site specific multipath effects, these errors are highly correlated over short times scales and can be eliminated by stochastic filtering and differencing of measurements from consecutive epochs. Based on measurements collected over several hours with widely varying orientations of the antenna, a spherical harmonics approximation of the phase pattern can be estimated in real-time in a Kalman filtering process. Compared to traditional field calibrations the automated calibration does not require a reference antenna, yields absolute phase patterns and benefits from a full and homogenous coverage of the entire antenna field of view. Phase patterns determined by this technique have been found to match those of anechoic chamber calibrations at the 1 mm level (Görres et al. 2004).

The IfE measurement robot with the S67-1575-14+CRG antenna is shown in Fig. 2. Since no suitable mock-up of the spacecraft environment could be made available, the test unit comprised only the antenna and choke ring. As a result, multipath or diffraction induced phase pattern variations caused by the vicinity of the antenna could not be incorporated into the ground calibration. While these effects have earlier been shown to be of relevance for the wing-mounted helix antenna of the GOCE spacecraft (Dilssner et al. 2006), they are expected to be less severe on CHAMP, GRACE and TerraSAR-X due to a more benign antenna design and accommodation.

Due to the passive nature of the antenna element, an external low noise amplifier (Spectrum Microwave 301-025105) was required, which was attached to the bottom side of a mounting plate connecting the robot and the choke ring. Even though a distortion of the phase pattern due to the asymmetric placement of the amplifier cannot be ruled out in principle, no obvious correlation with phase pattern variations could be detected in the test results. In total, four different samples of the S67-1575-14 antenna element from three manufacturing lots have been measured with the same choke ring to assess the repeatability of the phase pattern and the uncertainty of the calibration process.

Phase center offset and variation

Conceptually, the phase center offset (PCO) describes the difference between the mean center of the wave front and the ARP, while phase center variations (PCV) represent direction dependent distortions of the wave front. The

Table 1 Average phase center offset of S67-1575-14+CRG antenna and standard deviation based on automated field calibration of four individual units

Frequency	N (+y) (mm)	E (+x) (mm)	U (+z) (mm)
L1	1.49 ± 0.09	0.60 ± 0.12	−7.01 ± 0.48
L2	0.96 ± 0.26	0.86 ± 0.20	22.29 ± 0.44

carrier phase measurement can thus be described by the relation.

$$\Phi = |\boldsymbol{r}_{\mathrm{ARP}} + \Delta\boldsymbol{r}_{\mathrm{PCO}} - \boldsymbol{r}_{\mathrm{GPS}}| + \mathrm{PCV}(\boldsymbol{e}) + \cdots \approx |\boldsymbol{r}_{\mathrm{ARP}} - \mathbf{r}_{\mathrm{GPS}}| + \left[-\boldsymbol{e}^{T} \cdot \Delta\boldsymbol{r}_{\mathrm{PCO}} + \mathrm{PCV}(\boldsymbol{r})\right] + \cdots \quad (1)$$

where $\boldsymbol{r}_{\mathrm{ARP}}$ and $\boldsymbol{r}_{\mathrm{GPS}}$ denote the position of the receiver ARP and the GPS transmit antenna, respectively, $\boldsymbol{e}$ is the line-of-sight unit vector from the receiver to the satellite and ellipses (⋯) denote other terms in the measurement model such as clock offsets and atmospheric delays. In accord with established IGS conventions (Rothacher and Schmid 2006), the PCO is unambiguously determined by constraining the PCV in the boresight direction to zero. For completeness, we note that phase pattern corrections of the GPS transmit antenna are not explicitly accounted for in the above equation but can likewise be described by corresponding phase center offsets and variations.

As detailed in Table 1, the L1 and L2 phase centers of the S67-1575-14+CRG antenna are separated by roughly 30 mm and exhibit axial offsets of −7 mm and +22 mm from the adopted ARP. In addition the PCO exhibits an off-axis component of 1–2 mm. Phase center offsets for different test units vary by less than 1 mm, which indicates a good repeatability of both the calibration process and the antenna manufacturing.

As a result of the choke ring, the phase pattern variation exhibits a high level of rotational symmetry with average elevation dependence as shown in Fig. 3. For the ionosphere-free combination of L1 and L2 carrier phase measurements, phase center variations with peak values of ±10 mm are encountered at low and mid elevations. Azimuth variations for a fixed elevation, in contrast, are less than 1.3 mm (rms) for elevations above 10°. They can probably be neglected in absolute navigation but need to be accounted for in differential GPS applications (such as the TerraSAR-X/TanDEM-X relative navigation) in case of non-matching antenna alignments. The scatter among different antenna samples induces an rms uncertainty of 1–1.5 mm for the L1/L2 combination, which is less than the average receiver noise.

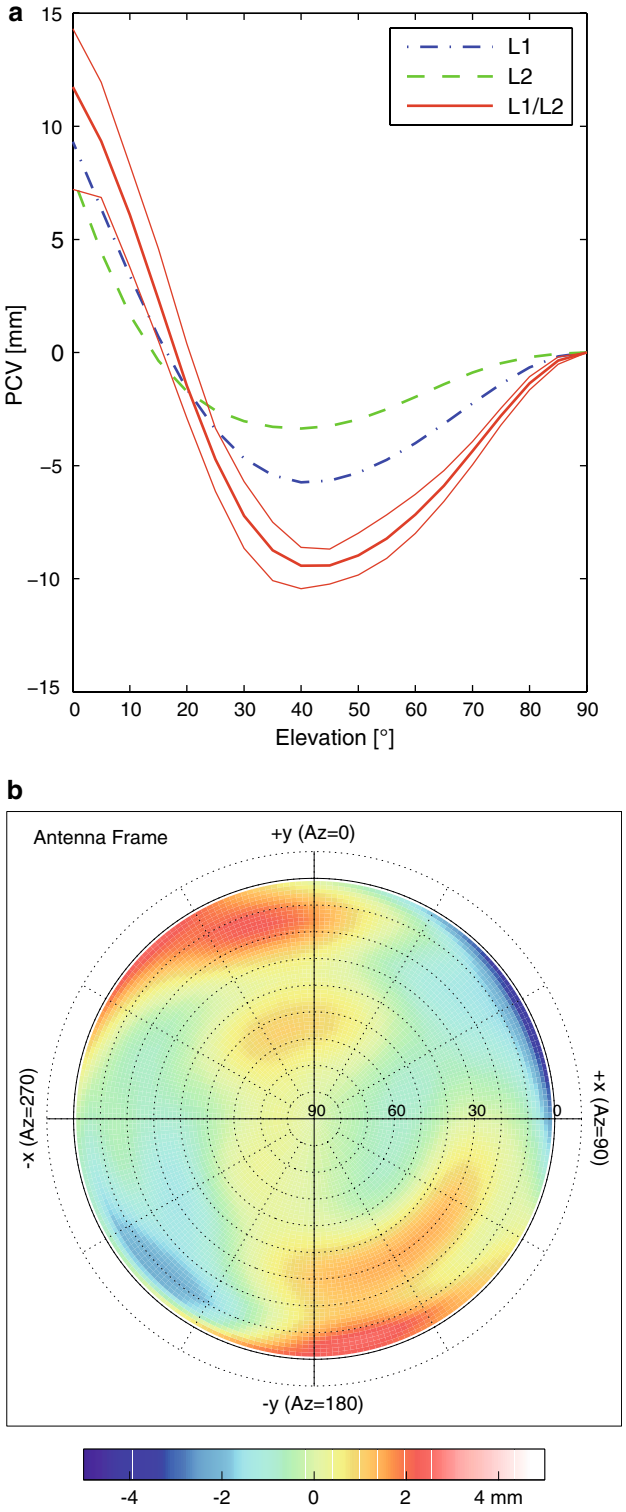

Fig. 3 Mean elevation dependency of the S67-1575-14+CRG phase pattern for L1 and L2 measurements as well as the ionosphere-free L1/L2 combination. (*top*, **a**). Besides the mean value (*bold red line*), the upper/lower bounds over all azimuth angles (*thins red lines*) are also shown for L1/L2. The azimuth variation relative to the mean pattern for L1/L2 is illustrated in the *bottom*, **b** image

In-flight calibration

Data sets

An in-flight calibration was independently carried out for the phase pattern of the "POD main" and "POD aux" antennas of TerraSAR-X (TSX) and the "GPS main" antenna of GRACE-B (GRB). These spacecraft are equipped with similar IGOR and BlackJack receivers which provide highly accurate, low noise code and carrier phase measurements (Montenbruck et al. 2006). In all cases 11 days of data were processed, covering days 270–280 of 2007 for the TerraSAR-X and GRACE-B main antennas and days 332–342 of 2007 for the TerraSAR-X auxiliary antenna. Due to receiver internal cross-talk, measurements of the BlackJack/IGOR receiver are known to be affected by systematic, multipath-like errors during activation of the occultation antenna (Montenbruck and Kroes 2003). Within the present study it has therefore been decided to ignore data from the trailing GRACE-A satellite, which was collecting occultation measurements of setting GPS satellites during the period of interest.

Precise GPS orbits and 30 s clock products were obtained from the Center for Orbit Determination in Europe (CODE; Hugentobler et al. 2006). While similar products are available from the International GNSS Service (IGS) since late 2006, the IGS clock solutions were found to be affected by small inconsistencies at integer 5 min epochs. These can readily be attributed to the imbalanced merging of 5 min and 30 s clock solutions from different analysis centers that destroys the short-term continuity of the resulting combined product. For the present study, the use of a self-consistent product from a single IGS analysis center was therefore preferred (Note: following Kouba (2008) based on a personal communication with G. Gendt, the clock problem has been largely corrected in the IGS 30 s products since January 2008).

For validation of the GPS based precise orbit determination solutions use was made of satellite ranging normal points collected by the International Satellite Laser Ranging Service (ILRS; Pearlman et al. 2002) on the days of interest.

Coordinates of the ARP in the spacecraft body frame are summarized in Table 2. Without loss of generality, the begin-of-life values have been adopted for TerraSAR-X. While it's center-of-gravity (CoG) shifts by roughly 10 mm/year in along-track direction, this motion cannot be discerned in the POD process or the satellite laser ranging (SLR) data validation. Radial and cross-track variations of the CoG, in contrast are confined to less than 0.5 mm. For the GRACE satellites, the CoG location is held fixed throughout the entire mission using adjustable trim masses. In addition to the ARP coordinates, Table 2 provides the boresight vector and the direction of the antenna azimuth origin (antenna + y axis) in the spacecraft frame. It may be noted that the TerraSAR-X main and auxiliary antennas exhibit a 90° azimuth offset as a result of a different mounting. For GRACE-B, details of the antenna mounting are no longer traceable and the same alignment as for the TerraSAR-X main antenna has been assumed. The orientation of the spacecraft body frame relative to the celestial reference frame is described by star sensor based attitude quaternions provided by the respective operators of the GRACE and TerraSAR-X missions.

Precise orbit determination

The GHOST GPS High-precision Orbit Determination Software Tools (Montenbruck et al. 2005) were used to compute reduced dynamic and kinematic position solutions of the GRACE and TerraSAR-X satellites. Both techniques make use of a least-squares adjustment but differ in the set of estimation parameters. While epoch-wise center-of-gravity positions are determined in the kinematic approach, an initial state vector and piece-wise constant empirical accelerations (at 10 min intervals) as well as a drag and radiation pressure coefficient are estimated in the reduced dynamic case. Aside from the aforementioned parameters, epoch-wise clock offsets and pass-by-pass carrier phase biases are adjusted in both solutions. A summary of the

Table 2 GPS antenna and satellite laser reflector position in the spacecraft body system relative to the center-of-gravity (CoG) for TerraSAR-X (E. Herbst, priv. comm.) and GRACE (Bettadpur 2004)

Spacecraft	Point	X (mm)	Y (mm)	Z (mm)	Boresight (+z)	Azimuth(+y)
TerraSAR-X	POD main antenna (ARP)	+1604.3	−16.8	−1065.2	(0, 0, −1)	(0, −1, 0)
	POD aux antenna (ARP)	+1234.3	−16.8	−1065.2	(0, 0, −1)	(−1, 0, 0)
	SLR reflector	−1307.7	−212.1	+953.8		
GRACE	GPS main antenna (ARP)	0.0	0.0	−444.0	(0, 0, −1)	(0, −1, 0)
	SLR reflector	+600.0	−327.5	+217.8		

Values for TerraSAR-X refer to the begin-of-life (wet mass). In addition, the direction of the antenna boresight and the azimuth origin ("North" direction) of the GPS antenna in the spacecraft body frame are specified

employed measurement and trajectory models is provided in Table 3. All GPS measurements were processed in batches of 24 h duration. To avoid the impact of GPS clock interpolation errors, the observations were sampled at 30 s intervals matching the epochs of the CODE ephemeris products.

In accord with current IGS processing standards, GPS satellite specific antenna offsets and phase patterns (Schmid et al. 2007) have been accounted for in the measurement model. Unfortunately, the calibration of GPS satellite antenna phase patterns based on terrestrial measurements is naturally restricted to boresight angles of 14°. In contrast to this, boresight angles of 15–17° are encountered in the processing of GPS measurements from LEO satellites at 500–1,300 km altitude. As a remedy, the transmit antenna phase center variation has been held constant at their published value for boresights above 14°. Even though dedicated calibrations of the GPS transmit antenna phase pattern using GRACE and Jason measurements have been reported by Bar-Sever et al. (2006), their results are incompatible with IGS conventions and data products. Therefore, they could not be utilized in this study.

Empirical phase pattern corrections

Following Eq. (1), any error

$$\Delta\mathrm{PCV}(\boldsymbol{e}) = \mathrm{PCV}_{\mathrm{true}}(\boldsymbol{e}) - \mathrm{PCV}_{\mathrm{model}}(\boldsymbol{e}) \quad (2)$$

in the assumed phase pattern will result in a corresponding change

$$\Delta(\Phi_{\mathrm{obs}} - \Phi_{\mathrm{model}}) = \Delta\mathrm{PCV}(\boldsymbol{e}) \quad (3)$$

in the difference of observed and modeled measurements prior to the least-squares orbit adjustment. Part of this difference will also show up in line-of-sight dependent post-fit residuals. Indeed, the mean values of the carrier phase residuals in a reduced dynamic orbit determination can often be seen to exhibit notable variations with azimuth and elevation (see, for example, Haines et al. 2004; Jäggi et al. 2007). These mean values can be interpreted as unmodeled phase patterns and can henceforth be taken into account as supplementary, empirical phase pattern corrections.

For the three antennas considered in this study, empirical phase pattern corrections have been derived from residuals of the reduced dynamic orbit determination taking into account the nominal phase center offset and variation from the ground calibration. To this end, the measurement residuals were sorted in azimuth/elevation bins of about 0.6×10^{-3} steradian ($1.5° \times 1.5°$ at low elevation). Daily statistics (mean, standard deviation and number of measurements) were stored for each bin and subsequently combined to obtain a mean value for the entire 11-day test period.

Results and discussion

Empirical phase pattern corrections derived from the carrier phase residuals of reduced dynamic orbit determinations are shown in Figs. 4 and 5 for TerraSAR-X

Table 3 Summary of the dynamical and measurement models used for the GPS based precise orbit determination and SLR orbit validation of GRACE and TerraSAR-X

Item	Description
GPS measurement model	Undifferenced ionosphere-free code and phase observations, corrected for approximate receiver clock offset; 5° cut-off
	Phase center offsets and variations of transmitter and receiver antennas
	Phase wind-up
	CODE GPS orbits and 30s clock solutions in IGS05 reference system
SLR measurement model	SLRF2005 coordinates
	Solid Earth and pole tides (IERS2005); GOT00.2 ocean loading
	Marini & Murray tropospheric delay model (IERS2005)
Gravitational forces	UT/CSR GGM01 model (100 × 100)
	Relativity solid-earth tides; pole tide; ocean tides (UT/CSR TOPEX_3.0)
	Luni-solar third body acceleration using low-accuracy analytical ephemerides
Non-gravitational forces	Jacchia-Gill atmospheric density model with daily $F_{10.7}$ and 3-hourly K_p values
	Cannon ball solar radiation pressure model with conical Earth shadow model (umbra, penumbra)
	Empirical accelerations in radial, along-track and cross-track direction at 10 min intervals
Reference frames	EME2000; IAU 1976 precession (Lieske model); IAU 1980 nutation (Wahr model); Earth orientation from IERS igs96p02 solution; spacecraft body frame orientation relative to EME2000 based on star sensor attitude determination

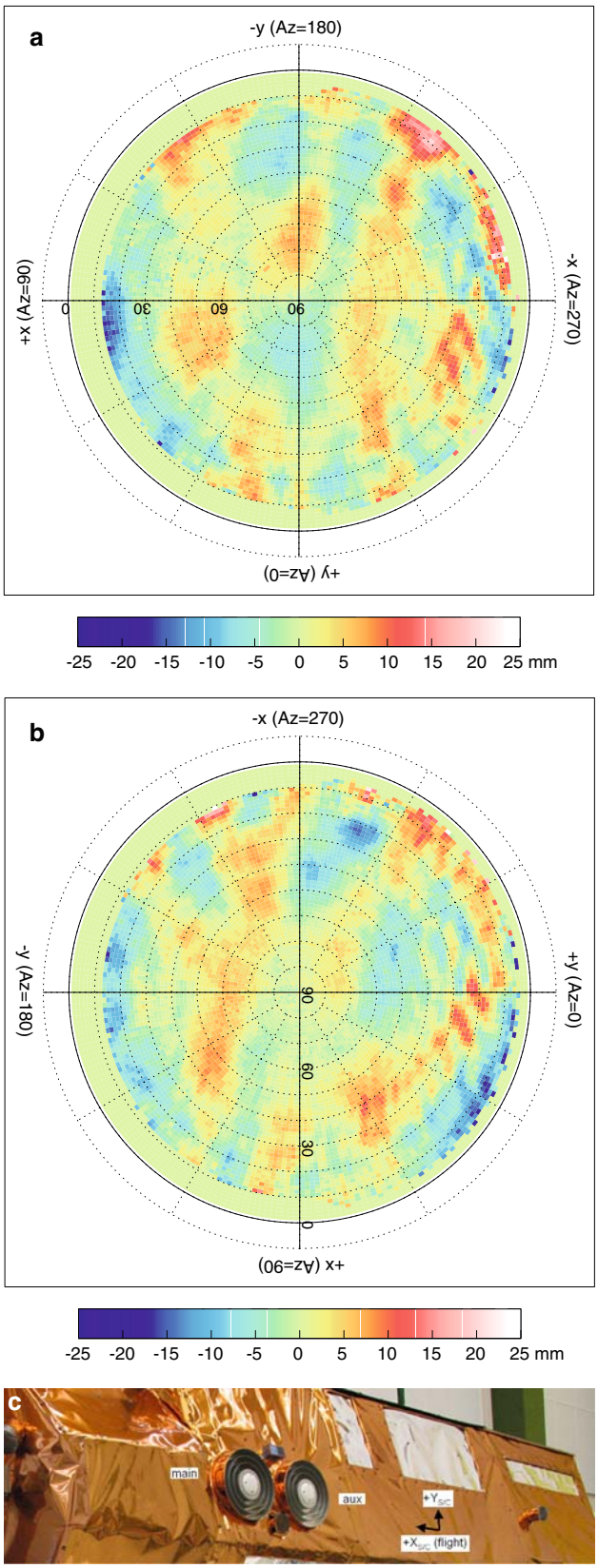

Fig. 4 Phase pattern corrections from ionosphere-free L1/L2 carrier ▶ phase residuals for the main (*top*, **a**) and auxiliary (*center*, **b**) POD antenna of Terra-SAR-X. The labeled axes in the satellite image denote the orientation of the spacecraft reference system. The phase pattern plots have been rotated such as to match the orientation of the antennas in the satellite image (*bottom*; courtesy EADS/IABG)

and GRACE-B, respectively. In addition, the figures provide a picture of the host satellite and the local antenna environment. The individual phase maps and axes refer to the antenna coordinate system but have been aligned with the actual antenna orientation in the satellite images.

The phase pattern corrections are typically confined to amplitudes of less than 10 mm for TerraSAR-X. Peak values of 15 mm at low elevations may in part be attributed to reflections from a slightly exposed S-band antenna (located between the main and auxiliary POD antennas and offset in the spacecraft $-Y_{S/C}$ direction) as well as nearby edges of the spacecraft structure in the $+X_{S/C}$ and $-Y_{S/C}$ direction of the POD main antenna. However, pronounced short scale variations (over bore-sight angle changes of $<10°$) are even encountered at elevations of 30° and azimuth directions in the ($-X_{S/C}$/$-Y_{S/C}$) quadrant of the spacecraft. These phase pattern distortions are most obvious for the auxiliary POD antenna but cannot be attributed to a reflecting structure on the satellite surface. A possible cross-talk of amplified signals from the antenna of another, single-frequency GPS receiver onboard TerraSAR-X might be an alternative explanation but cannot be substantiated due to lack of test opportunities at this stage of the mission.

For GRACE-B the amplitude of the phase pattern corrections is generally lower (typically <5 mm) than for TerraSAR-X. Evidently, GRACE-B benefits from the fact that its zenith-facing side is fully covered with plane solar cells, while TerraSAR-X is packed in thermal insulation foil that creates a more irregular surface structure. Closely matching phase patterns have previously been obtained for GRACE-B by Jäggi et al. (2007) with a different data set (days 236–298 of 2003) and different software (Bernese GPS Software, Dach et al. 2007) but without knowledge of an a priori ground calibration. The similarity of both results confirm the constancy of the phase pattern distortions and the general applicability of the derived measurement corrections.

Table 4 summarizes the magnitude of the carrier phase residuals and the difference of kinematic and reduced dynamic orbit determination solutions considering four different types of phase center corrections for each antenna. The largest residuals of about 10 mm for undifferenced ionosphere-free carrier phase measurements are obtained, if the phase center is identified with the antenna reference point. Application of individual L1 and L2 phase center offsets further reduces the residuals as does the additional consideration of the phase center variation determined in

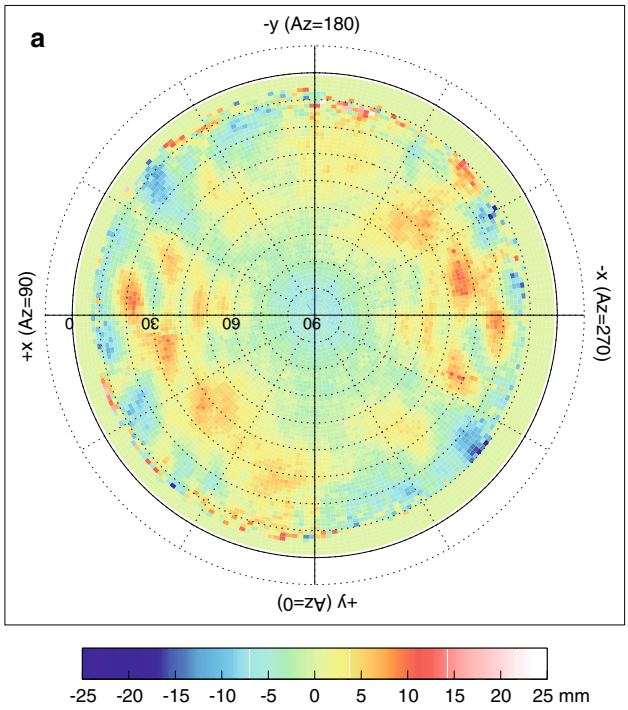

Fig. 5 Phase pattern corrections from ionosphere-free L1/L2 carrier phase residuals for the POD antenna of GRACE-B (*top*). The labeled axes in the satellite image denote the orientation of the spacecraft reference system. The phase pattern plot has been rotated such as to match the orientation of the antenna in the satellite image (*bottom*; courtesy EADS/IABG)

the ground calibration. Finally, residuals down to about 4 mm are obtained in a reduced dynamic solution when taking into account the additional empirical phase pattern correction from the in-flight calibration. This is close to the thermal noise of the employed receiver (2–3 mm) and is indicative of the excellent quality of the CODE 30 s GPS clock solutions.

In the kinematic solutions, residuals are generally smaller due to the larger number of estimation parameters and associated degrees of freedom. However, the same trend and improvement as for the reduced dynamic solution may be observed when applying successively better phase pattern corrections. For GRACE-B, systematically smaller residuals are obtained than for TerraSAR-X despite the use of very similar receivers and identical antennas. Besides the lower distortion of the phase pattern by the local environment, this may be due to the smaller average number of tracked satellites per epoch (7 versus 9). Due to the reduced redundancy of measurements at a given epoch, smaller residuals are thus obtained but measurement errors are more likely to be absorbed into the estimated positions.

Along with the overall reduction of the carrier phase residuals in kinematic and reduced dynamic solutions, the consistency of both solutions clearly improves when better phase center corrections are applied (cf. Table 4). In the absence of any corrections a pronounced radial bias of the kinematic position solutions can be observed. Consideration of the nominal L1 and L2 phase center shift changes the height of the kinematic positions by about 5.1 cm. This value closely matches the ionosphere-free linear combination.

$$\begin{aligned}\Delta z &= 2.5457 \cdot \Delta z_{\mathrm{PCO,L1}} - 1.5457 \cdot \Delta z_{\mathrm{PCO,L2}} \\ &= -52.3 \text{ mm}\end{aligned} \quad (4)$$

of the individual offsets and suggests the suitability of an effective "ionosphere-free" phase center for first order antenna offset corrections. This may be helpful for use in heritage orbit determination software that does not support a dedicated phase center modeling and to properly interpret past mission results obtained with lacking phase center information. Due to the employed normalization of the phase center variation (zero PCV in the boresight direction), the average PCV differs from zero and its application in the orbit determination results in a further shift (3–5 mm) of the kinematic position solutions. A mm level consistency of the kinematic and reduced dynamic altitudes is finally achieved when considering also the empirical phase pattern corrections (Table 4).

Since the in-plane components of the kinematic position errors exhibit a pronounced once-per-rev pattern when expressed in a co-moving orbital frame, a different set of base vectors aligned with the line-of-nodes (N), the direction of highest latitude (K) and the orbital plane normal (W) has been chosen for the comparison of kinematic and reduced dynamic position solutions. Sample time series for the TerraSAR-X POD main antenna obtained before and after application of the empirical phase pattern corrections are shown in Fig. 6. The correction clearly reduces the noise of the kinematic position solution over typical

Table 4 Carrier phase residuals (rms) and difference of kinematic (KIN) and reduced dynamic (RD) orbit determination solutions

Spacecraft, antenna	Offset and pattern	Residuals KIN (mm)	Residuals RD (mm)	KIN-RD rms (cm)	KIN-RD mean radial (cm)
TSX, main	ARP	5	10	6.6	−4.3
	+PCO ground calib.	5	7	4.8	+0.8
	+PCV ground calib.	4	6	4.2	−0.4
	+in-flight correction	3	4	3.2	−0.1
TSX, aux	ARP	5	10	6.6	−4.1
	+PCO ground calib.	5	7	5.0	+0.9
	+PCV ground calib.	4	6	4.3	−0.6
	+in-flight correction	3	4	4.0	−0.1
GRB, main	ARP	3	8	6.7	−4.2
	+PCO ground calib.	3	5	4.8	+0.9
	+PCV ground calib.	3	6	4.9	−0.1
	+in-flight correction	2	4	4.7	−0.1

Table 5 Satellite laser ranging residuals for different reduced dynamic orbit determination solutions of TerraSAR-X and GRACE-B

Spacecraft, antenna	Offset and pattern	High quality sites			All sites		
		Mean (cm)	RMS (cm)	*N*	Mean (cm)	RMS (cm)	*N*
TSX, main	ARP	−0.3	1.6	1,931	−0.3	2.5	2,276
	+PCO ground calib.	−0.2	1.5		−0.3	2.1	
	+PCV ground calib.	−0.2	1.4		−0.2	2.1	
	+in-flight correction	−0.3	1.4		−0.3	2.2	
TSX, aux	ARP	0.1	1.7	1,517	+0.4	2.5	2,154
	+PCO ground calib.	0.1	1.4		+0.4	2.3	
	+PCV ground calib.	0.1	1.3		+0.4	2.3	
	+in-flight correction	0.0	1.3		+0.2	2.2	
GRB, main	ARP	−0.4	1.6	687	−0.5	2.7	841
	+PCO ground calib.	−0.4	1.1		−0.4	2.5	
	+PCV ground calib.	−0.3	1.2		−0.4	2.5	
	+in-flight correction	−0.4	1.1		−0.4	2.4	

The columns provide the 11 days mean and rms of the SLR residuals as well as the number of normal points considering all observations above 10° elevation. Separate results are given for high-quality sites (bias and noise <3 cm) and the full set of all SLR stations

time scales of 30 min. The long-term variation, in contrast, is identical in both cases and can best be attributed to GPS ephemeris errors (and possibly phase pattern errors) at a level of 1–2 cm. These errors induce systematic offsets in the kinematic position that depend only on the varying constellation of tracked satellites but bear no other relation with the orbit of the LEO satellite.

Other than the kinematic solutions, the reduced dynamic solutions are fairly insensitive to changes in the applied phase pattern corrections and varied by less than 1.5 cm (3D rms) in the analyzed test cases. While the mean radial position components of all solutions agreed to better than 1 mm rms, systematic shifts of up to 1 cm in the cross-track component were observed when applying different phase patterns. Such biases are likewise encountered in kinematic solutions (albeit more pronounced) and reflect a lack of stability of the reduced dynamic solutions perpendicular to the orbital plane.

For an independent assessment of the various reduced dynamic orbit determination results, we analyzed the residuals of satellite laser ranging measurements relative to the GPS based orbit solutions (Table 5). In view of obvious performance differences among the available SLR stations we provide separate results for the full set of observatories and for a subset of stations with measurement biases and standard deviations of less than 3 cm. These high-quality stations (including, in particular, Herstmonceaux, Graz, Greenbelt, Mount Stromlo, Yarragadee, and Zimmerwald) contribute more than 75% of the available observations and fit the GPS orbits with a typical accuracy of 1.5 cm. The

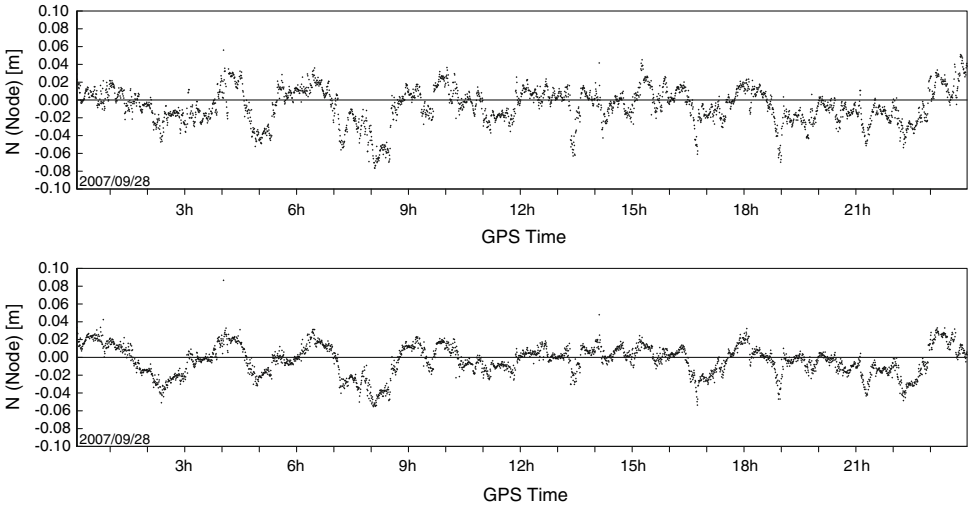

Fig. 6 Differences of kinematic and reduced dynamic positions of TerraSAR-X for day 271 of 2007 before (*top*) and after (*bottom*) application of phase pattern corrections from the in-flight calibration. The graphs show the one-dimensional projection of the in-plane position difference on an axis parallel to the line-of-nodes

full set in contrast, yields about 50% larger rms residuals of 2–2.5 cm. While a slightly inferior quality of the ARP-only solution can be confirmed from the analysis of the SLR residuals, the measurement (and modeling) accuracy is apparently insufficient to discriminate a possible benefit of ground or in-flight calibrated phase patterns in the reduced dynamic orbit determination.

As a final test we assessed the capability of recovering the total phase pattern relative to the ARP from an in-flight analysis of carrier phase residuals, if no a priori knowledge of the phase center offset and variation is available from the ground calibration. The resulting pattern for the POD main antenna of TerraSAR-X is shown in Fig. 7 along with the cumulative effects of the PCO, PCV and in-flight corrections discussed previously. A constant offset of about 25 mm may be noted in the comparison of both patterns. This offset is compensated for by a corresponding change in the estimated carrier phase biases and does not affect the estimated position solutions. Furthermore, the in-flight calibration of the total pattern yields a flatter overall pattern with a less pronounced elevation dependence than the calibration with a priori ground pattern information.

Due to the estimation of pass-dependent biases, phase pattern variations perpendicular to the flight direction are, to a fair extent, absorbed in the biases and the in-flight calibration reveals primarily the phase pattern variations in the along-track direction. This problem is specific to satellites maintaining a near constant orientation relative to the orbital frame (such as CHAMP, GRACE, and GOCE), but does not impact on the suitability of the resulting phase pattern corrections. For TerraSAR-X, kinematic and reduced dynamic solutions computed with the total phase pattern calibration agree to roughly 3.6 cm (3D rms), which is better than the ground-only calibration and only moderately worse than the ground-plus-in-flight calibration.

In case of satellites performing large yaw angle variations one may expect a better recovery of the total phase pattern since the apparent tracks of the GPS satellites in the antenna reference system vary throughout the course of the mission. Indeed, the in-flight calibration of the Jason-1 antenna (Luthke et al. 2003, Haines et al. 2004) exhibits no indications of a flattened antenna pattern. However, final conclusions cannot be drawn in this case due to the lack of suitable ground calibration data.

Summary and conclusions

Phase pattern variations of a spaceborne GPS antenna have been determined and their impact on the precise orbit determination of LEO satellites has been analyzed. Due to lack of dynamical constraints, kinematic solutions for the spacecraft center-of-gravity depend critically on the assumed phase center location and antenna pattern, while dynamically constrained orbit determinations provide stable and accurate height solutions. The radial difference of kinematic and reduced dynamic solutions can thus provide a useful indication of possible phase center mismodeling. In the absence of other information, an effective ionosphere-free phase center can be established and used as an alternative to a more rigorous antenna model.

Ground calibrations of the antenna assembly are recommended in order to obtain the best available a priori phase pattern information for missions with stringent orbit determination requirements. In the case of GRACE and TerraSAR-X, a 1.5 cm rms agreement of GPS based reduced dynamic solutions with SLR observations from high grade stations and a 4–5 cm (3D rms) consistency of kinematic and reduced dynamic orbits was obtained with application of antenna phase patterns from a ground calibration.

However, systematic variations of the carrier phase residuals with azimuth and elevation are evident in both

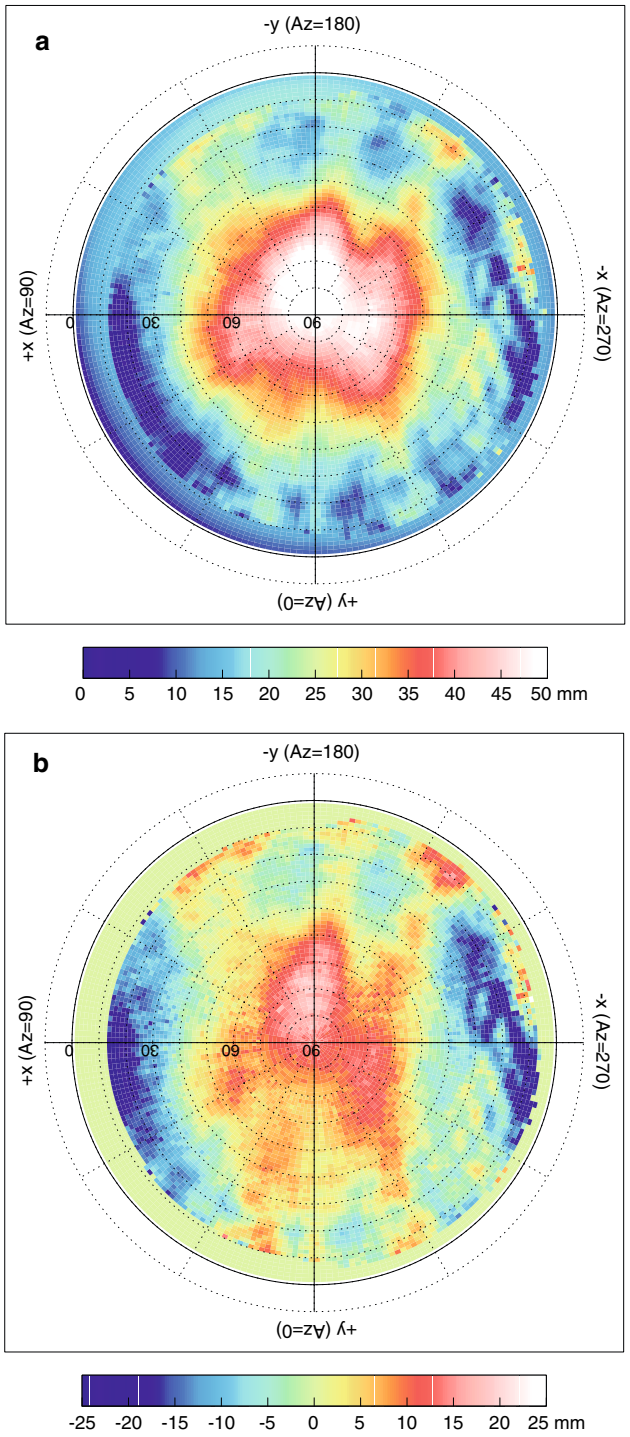

Fig. 7 Total phase pattern of the TerraSAR-X main POD antenna relative to the antenna reference point as derived from an in-fight calibration with (*top*) and without (*bottom*) a priori knowledge of the phase center offset and variation from the ground calibration. Note the different color scales

missions which indicates distortions of the phase pattern by the near-field spacecraft structure. This impact is most obvious for TerraSAR-X which is covered by mylar insulation foil, but less pronounced for GRACE with a top surface made up of solar cells. Phase center correction maps have been derived for three different antennas on TerraSAR-X and GRACE-B based on the average carrier phase residuals over an 11-day period. It is shown that these maps can further improve the consistency of kinematic and reduced dynamic solutions (down to the 3 cm level) as well as the goodness-of-fit of carrier phase measurements (down to 4 mm for reduced dynamic solutions). This is of particular interest for gravity science missions such as CHAMP or GOCE, where systematic errors in the kinematic position solutions might lump into errors of low order gravity field coefficients. Furthermore, the in-flight calibration will be of benefit for a concise modeling of differential carrier phases in the relative navigation and baseline reconstruction of the TerraSAR-X/TanDEM-X formation.

Despite promising results, the present analysis still suffers from an incomplete knowledge of the GPS satellite antenna pattern. A fully consistent calibration of LEO receiver antennas and GPS transmit antennas at large boresight angles will be required to reduce prevailing systematic modeling errors and to further increase the achievable LEO POD accuracy. In turn, a combined adjustment of LEO satellite orbits and GPS orbits might, in the future, help to further improve the quality of GPS ephemeris products.

Acknowledgments The IGOR receiver, choke rings and SLR reflector of TerraSAR-X have been contributed by the GeoForschungsZentrum (GFZ), Potsdam, to enable a high precision orbit determination of this spacecraft. Precise GPS ephemerides for use within this study have been obtained from the Center for Orbit Determination in Europe at the Astronomical Institute of the University of Bern (AIUB). Satellite laser ranging measurements of the GRACE and TerraSAR-X were provided by the International Laser Ranging Service (ILRS). The support of the above institutions is gratefully acknowledged.

References

Bar-Sever Y, Bertiger W, Byun S, Desai S, Haines B, Hajj G (2006) Calibrating the GPS satellites transmit antenna. In: IGS Workshop 2006, Darmstadt, pp 8–11

Bettadpur S (2004) Gravity recovery and climate experiment product specification document. GRACE 327-720 (CSR-GR-03-02), Rev 4.2, August 2, 2004, Center for Space Research, The University of Texas at Austin

Dach R, Hugentobler U, Fridez P, Meindl M (2007) Bernese GPS Software Version 5.0, University of Bern

Dilssner F, Seeber G, Schmitz M, Wübbena G, Tosos G, Maeusli D (2006) Characterisation of GOCE SSTI Antennas. Zeitschrift für Geodäsie. Geoinformation Landmanagement 131:61–71 (Zfv)

Görres B, Campbell J, Siemes M, Becker M (2004) New anechoic chamber results and comparison with field and robot techniques. In: Presented at the IGS Workshop 2004, Bern, Switzerland

Jäggi A, Hugentobler U, Bock H, Beutler G (2007) Precise orbit determination for GRACE using undifferenced or doubly differenced GPS data. Adv Space Res 39:1612–1619. doi: 10.1016/j.asr.2007.03.012

Kouba J (2008) A simplified yaw-attitude model for eclipsing GPS satellites. GPS Solut. doi:10.1007/s10291-008-0092-1

Luthke SB, Zelensky NP, Rowlands DD, Lemoine FG, Williams TA (2003) The 1-centimeter orbit: Jason-1 precision orbit determination using GPS, SLR, DORIS, and Altimeter data. Mar Geod 26:399–421. doi:10.1080/714044529

Haines B, Bar-Sever Y, Bertiger W, Desai S, Willis P (2004) One-centimeter orbit determination for Jason-1: new GPS based strategies. Mar Geod 27(1–2):299–318. doi:10.1080/01490410490465300

Hugentobler U, Meindl M, Beutler G, Bock H, Dach R, Jäggi A et al (2006) CODE IGS analysis center technical report 2003/04. In: Gowey k (ed) IGS technical reports 2003/04. IGS Central Bureau, JPL, CA

Kang z, Tapley B, Bettadpur S, Ries J, Nagel P, Pastor R (2006) Precise orbit determination for the GRACE mission using only GPS data. J Geod 80:322–331

Montenbruck O, Kroes R (2003) In-flight performance analysis of the CHAMP BlackJack receiver. GPS Solut 7:74–86. doi:10.1007/s10291-003-0055-5

Montenbruck O, van Helleputte T, Kroes R, Gill E (2005) Reduced dynamic orbit determination using GPS code and carrier measurements. Aerosp Sci Technol 9(3):261–271. doi:101016/jast200501003

Montenbruck O, Garcia-Fernandez M, Williams J (2006) Performance comparison of semi-codeless GPS receivers for LEO satellites. GPS Solut 10:249–261. doi:101007/s10291-006-0025-9

Pearlman MR, Degnan JJ, Bosworth JM (2002) The international laser ranging service. Adv Space Res 30(2):135–143. doi:10.1016/S0273-1177(02)00277-6

Rothacher M, Schmid R (2006) ANTEX: The Antenna Exchange Format Version 1.3, 20 September 2006

Schmid R, Rothacher M, Thaller D, Steigenberger P (2005) Absolute phase center corrections of satellite and receiver antennas—impact on global GPS solutions and estimation of azimuthal phase center variations of the satellite antenna. GPS Solut 9(4):283–293. doi:10.1007/s10291-005-0134-x

Schmid R, Steigenberger P, Gendt G, Ge M, Rothacher M (2007) generation of a consistent absolute phase center correction model for GPS receiver and satellite antennas. J Geod 81(12):781–798. doi:10.1007/s00190-007-0148-y

Sensor Systems (2003) Outline drawing L1/L2 GPS antenna passive 1575/1227 MHz (S67-1575-14); Doc. No. 0575141A #4 SA 10-31-03; Sensor Systems Inc

Wübbena G, Schmitz M, Menge F, Böder V, Seeber G (2000) Automated absolute field calibration of GPS antennas in real-time. In: Proc ION GPS-2000, pp 2514–2522

Author Biographies

Oliver Montenbruck is head of the GNSS Technology and Navigation Group at DLR's German Space Operations Center, where he started to work as a flight dynamics analyst in 1987. His current research activities comprise spaceborne GNSS receiver technology, autonomous navigation systems, spacecraft formation flying and precise orbit determination.

Miquel Garcia-Fernandez holds a PhD in Aerospace Science and Technology from UPC, Barcelona. After a post-doctoral program in the University of Kyoto, he joined DLR in 2005. Since 2008 he works at Starlab S.L., Barcelona, as Senior Researcher. The focus of his work is the processing of GNSS signals and mea-surements for scientific applications.

Yoke T. Yoon received the PhD degree in Aerospace Engineering Sciences from the University of Colorado at Boulder. In 2004, she joined the DLR's German Space Operations Center to design, maintain and support the operational Precise Orbit Determination system for the TerraSAR-X mission. Since April 2008, she is a staff member at DEIMOS Space S.L., Tres Cantos.

Steffen Schön is professor for positioning and naviga-tion at Leibniz University Hannover. His current re-search interests are indoor positioning and navigation with high sensitivity GNSS and MEMS IMU, improve-ment of the stochastic model of GNSS observations as well as the correction and assessment systematic errors in GNSS, like e.g., absolute antenna calibration.

Adrian Jäggi is a senior researcher at the Astronomical Institute ofthe University of Bern (AIUB). The focus of his research lies in the area of orbit and gravity field determination.